scientific reports

Check for updates

OPEN

Preoperative comprehensive risk estimation for axillary lymph node metastasis in breast cancer: development and verification of a network-based prediction model

Baoqi Sun[1,4], Guangdong Shao[2,4]✉, Mingming Shi[2], Zenggang Sun[3], Xiaolin Wang[2], Yining Song[2], Zheng Sun[2], Zhanjie Jin[2], Chunhong Xu[2] & Guolou Li[2]

To prevent the overaggressive treatment of axillary lymph nodes (ALNs) in breast cancer, it is necessary to develop a convenient analysis method that accurately and comprehensively reflects whether ALNs are metastatic or nonmetastatic. We retrospectively analyzed data from patients who underwent surgery for breast cancer at the Weifang Hospital of Traditional Chinese Medicine between January 2019 and June 2023. Binary logistic regression analysis was used to predict the metastasis status of ALNs. The developmental data set included 531 patients (January 2019–June 2023). The validation set included separate data points (n = 178, January 2019–June 2023). Multivariate analysis revealed that positive findings on breast physical examination, ultrasound grades of ALNs, lymphovascular invasion, and Her-2 status had significant predictive value for metastatic ALNs. Based on these findings, a 5-grade risk scoring system and 3-level management recommendations were developed. The risk of metastasis ranged from 11.25 to 93.46%, which was positively correlated with an increase in risk grade. The areas under the curve of the development and validation sets were 0.895 and 0.865, respectively. Ultimately, a convenient, accurate and comprehensive web-based predictive model was constructed using various breast cancer clinical, imaging and pathological criteria to stratify ALNs according to the metastasis probability.

Keywords Breast cancer, Axillary lymph node status, Preoperative estimation, Metastasis probability, Network model

Abbreviations

ALNs	Axillary lymph nodes
ALND	Axillary lymph node dissection
AUC	Area under the curve
CQ	Central quadrant
ER	Estrogen receptor
FNA	Fine-needle aspiration
FNAC	Fine-needle aspiration cytology
FISH	Fluorescence in situ hybridization
Her-2	Human epidermal growth factor receptor 2
IHC	Immunohistochemistry
LOQ	Lower outer quadrant

[1]Department of Ophthalmology, Affiliated Hospital of Shandong Second Medical University, No. 288 Shengli East Street, Kuiwen District, Weifang City 261000, Shandong Province, China. [2]Department of Thyroid and Breast Diagnosis and Treatment Center, Weifang Hospital of Traditional Chinese Medicine, Shandong Second Medical University, No. 1055 Weizhou Road, Kuiwen District, Weifang City 261000, Shandong Province, China. [3]Shandong Second Medical University, No. 288 Shengli East Street, Kuiwen District, Weifang City 261000, Shandong Province, China. [4]Baoqi Sun and Guangdong Shao contributed equally to this work and share first authorship. ✉email: 15762509159@163.com

LIQ	Lower inner quadrant
LVI	Lymphovascular invasion
MQ	Multiple quadrant
MSKCC	Memorial Sloan-Catelyn Cancer Center
NLR	Neutrophil to lymphocyte ratio
PR	Progesterone receptor
PLR	Platelet lymphocyte ratio
ROC	Receiver-operating characteristic
SLNB	Sentinel lymph node biopsy
SLNs	Sentinel lymph nodes
UOQ	Upper outer quadrant
UIQ	Upper inner quadran

Breast cancer is a common malignant tumor that poses a significant threat to human health[1]. As the first station of breast lymphatic drainage, the axillary lymph node (ALN) plays a crucial role in breast cancer. Precise assessment and management of ALNs are of utmost importance for regional disease control, accurate staging of breast cancer, individualized treatment decision-making, and reliable prognosis evaluation[1,2]. Currently, sentinel lymph node biopsy (SLNB) and axillary lymph node dissection (ALND) are clinically recognized as the gold standard procedures for assessing the pathological status of ALNs (pNx) in early-stage breast cancer[2,3]. However, both of these methods are invasive, and complications associated with axillary surgery, such as upper limb lymphedema, shoulder and back pain, arm numbness, and reduced arm strength, are inevitable, significantly impacting patients' postoperative quality of life[4,5]. In recent years, the results of several rigorously designed prospective clinical trials, including the SOUND (NCT02167490), BOOG-2013-08 (NCT02271828), INSEMA (NCT02466737), and SOAPET (NCT04072653) trials, have been published. These trials investigated the feasibility of de-escalation surgical approaches for managing ALNs. Additionally, the KEYNOTE-522 study explored the efficacy and safety of novel neoadjuvant treatment regimens for patients with early-stage triple-negative breast cancer, with all reporting positive efficacy data[6–10]. In this context, current clinical practice demands a more rigorous and scientific approach for the preoperative assessment of ALN status in breast cancer patients, to enable the development of more personalized and precise treatment plans.

Currently, the most commonly used non-invasive methods for clinically assessing the status of of ALN include physical examination and ultrasonography. Compared to traditional physical examination, ultrasonography, with its high-resolution imaging technology, offers a more detailed visualization of the morphological characteristics of ALNs, such as size, shape, boundary clarity, and internal echo properties, thereby enhancing diagnostic accuracy. However, ultrasonography is limited to providing information on lymph node morphology and is subject to operator dependence and subjectivity, which can compromise its accuracy[11,12]. Although the application of ultrasound-guided fine-needle aspiration cytology (FNAC) greatly makes up for the deficiencies of ultrasonographic diagnosis, the limited number of specimens obtained by fine-needle aspiration (FNA) may not fully reflect the extent of the disease, and the diagnosis is heavily reliant on the experience of the operator and pathologist, leading to a high degree of uncertainty[13,14]. To overcome the limitations of ultrasound diagnosis, multiple medical centers have developed a series of prediction models, such as the Memorial Sloan Kettering Cancer Center (MSKCC) model and SCH model based on breast tumor pathology features, as well as radiomics models based on PET-CT or breast MRI[11,15–17]. Although these predictive models largely mitigate the issues of operator dependence and subjectivity, they are characterized by incomplete coverage of predictive variables, high costs, procedural complexity, and limited popularizability, which restrict their clinical application[12,18].

In practical clinical work, clinicians often need to comprehensively assess a variety of risk factors associated with lymph node metastasis when evaluating the status of ALNs in breast cancer patients. These include physical examination results, imaging features of the breast and ALNs (tumor size, tumor laterality, tumor location, diffuse distribution, multifocality, cluster calcification, etc.), pathological features of breast tumors (lymphovascular invasion (LVI), histologic grade, estrogen receptor (ER), progesterone receptor (PR), human epidermal growth factor receptor 2 (Her-2) status, Ki-67 expression, etc.), and nonspecific systemic inflammatory markers (neutrophil to lymphocyte ratio (NLR) and platelet lymphocyte ratio (PLR), among others)[15,19–22]. Unfortunately, at present, we still lack a pragmatic and convenient model to comprehensively represent the overall significant features of ALNs. In view of this, this study intends to develop and verify such a web-based prediction model, thereby achieving hierarchical management of ALNs in breast cancer, fulfilling the purpose of precision medical treatment, and improving the patient's quality of life.

Materials and methods

This retrospective study was carried out in line with the moral standards stipulated in the Helsinki Declaration and the International Ethics Guide for Human Biomedical Research issued by the International Committee of Medical Scientific organizations. It was approved by the Medical Ethics Committee of Weifang Hospital of Traditional Chinese Medicine. The data collected in this study were all tested by Weifang Hospital of Traditional Chinese Medicine.

Study population

Clinical data (sex, age, menstrual state, findings on breast physical examination, ultrasound grades of ALNs, tumor imaging size, tumor laterality, tumor location, diffuse distribution, multifocality, cluster calcification, histologic grade, ER, PR, Her-2 state, Ki-67, LVI, neutrophil count, lymphocyte count and platelet count) from 1022 patients with breast cancer treated in our hospital from January 2019 to June 2023 were collected. After excluding patients who did not meet the criteria for admission, 710 patients were ultimately enrolled.

The inclusion criteria were as follows: 1) Invasive breast cancer confirmed pathologically; 2) ALND or SLNB surgery having been performed; 3) Availability of histopathology and immunohistochemistry results for the surgical specimen; 4) Assessment of ALN status and breast masses by ultrasound and mammography within one week prior to biopsy; and 5) Completion of routine blood tests at our hospital with results available before biopsy.

The exclusion criteria were as follows: 1) Incomplete medical records; 2) patients who had undergone neoadjuvant therapy; 3) patients with bilateral or recurrent breast cancer; 4) patients undergoing palliative surgery; 5) patients with other types of malignant tumors; 6) patients with acute or chronic infections and hematological diseases; 7) patients with a history of axillary surgery; and 8) patients who were taking antibiotics, immunosuppressants, or hormone drugs before routine blood tests.

Breast physical exam

All patients underwent a breast physical examination before the relevant auxiliary examination, and the positive breast signs included pathological nipple discharge, asymmetric thickening or nodularity, skin changes (peau d'orange, dimple sign, erythema, nipple excoriation, scaling, eczema, rupture), and secondary inverted nipples[3].

Calculation of inflammatory indices

Peripheral venous blood was taken from the upper limb on an empty stomach before biopsy and sent to the laboratory department of our hospital for determination by an automatic hematology analyzer. The neutrophil (N), lymphocyte (L) and platelet (P) counts in the blood results were recorded. NLR = N/L; PLR = P/L[23,24].

Ultrasonic evaluation

Two radiologists (with 15 and 10 years of experience in breast ultrasonography, respectively) performed ultrasound evaluation of the ALNs status and breast masses before biopsy. The image features of the ALNs status and masses were observed, measured and recorded. Tumor size was expressed as the longest diameter (cm) of the mass. Tumor laterality was recorded as left breast or right breast. Tumor location was recorded as upper outer quadrant, UOQ; lower outer quadrant, LOQ; upper inner quadrant, UIQ; lower inner quadrant, LIQ; central quadrant, CQ or multiple quadrant, MQ (the mass crosses two or more quadrants). The diffuse distribution of the mass was recorded as Yes or No. The multifocality of the mass was recorded as Yes or No. Multifocality was defined as foci of carcinoma separate from the primary tumor or a mass with diffuse distribution; no distinction was made between multifocality or multicentricity[15].

The ultrasound grade of ALNs was divided into a negative group (including Types 1, 2, 3, and 4) and a positive group (including Types 5 and 6) based on cortical morphologic features. The cortical morphologic features of each type of lymph node were defined as follows: Type 1, hyperechoic with no visible cortex; Type 2, thin (< 3 mm) hypoechoic cortex; Type 3, hypoechoic cortex thicker than 3 mm; Type 4, generalized lobulated hypoechoic cortex; Type 5, focal hypoechoic cortical lobulation; and Type 6, totally hypoechoic node with no hilum[25]. When multiple types of lymph nodes were present in the same patient, the one with the highest grade was selected for inclusion.

Mammography evaluation

The patients underwent mammography before breast biopsy, and each breast was routinely photographed in 2 positions, namely, the craniocaudal position and mediolateral oblique position. A double-blind analysis was conducted by two radiologists (with 5 and 10 years of experience in mammography, respectively) to analyze the mammography features. They reached consensus through consultation when different opinions were expressed. In this study, the image features of abnormal calcification in the breast were defined as 1) amorphous calcification of segment, line and cluster distribution; 2) rough heterogeneous calcification of single cluster distribution; and 3) fine pleomorphic calcification[26].

Surgery procedure for ALNs

The surgical methods for assessing ALNs include SLNB and ALND. For patients with clinically node-negative (cN0) status, ALNs were pathologically assessed using either SLNB alone or a combination of SLNB and ALND. For patients with clinically node-positive (cN1 +) status, ALNs were assessed using ALND. The sentinel lymph nodes (SLNs) were identified using blue dye and 99 m-Technetium sulfur colloid. In the protocol, an SLN was defined as any blue-stained node, any node with a blue-stained lymphatic channel leading directly to it, any node with a radioactive count at least 10% of the most radioactive node, or any pathologically palpable node. For patients with no more than two positive lymph nodes identified by SLNB, the decision to perform axillary dissection or not depended on the type of operation (breast-conserving therapy or mastectomy) and individual pathological characteristics [27].

Criteria for evaluating ALNs status

The final status (metastatic or nonmetastatic) of ALNs was postoperatively examined using serial sections with hematoxylin & eosin (H&E) staining. Macrometastases (> 2 mm cancer foci) or micrometastases (0.2–2 mm cancer foci) of ALNs were considered metastatic. It should be noted that the isolated tumor cells (ITCs, < 0.2 mm) were considered negative in the final statistical analysis[11,17].

Histopathological analysis

Breast specimens were analysed by 2 pathologists with 20 and 15 years of experience in breast disease, respectively. The pathological features included LVI status, histologic grade, ER status, PR status, Her-2 status and Ki-67 expression. The cutoff value of high expression of ER was based on the positive nuclear staining of

over 10% of the tumor cells[26]. The cutoff value of low expression of ER was based on the proportion of positive nuclear staining of tumor cells ≥ 1% and ≤ 10%[26]. The cutoff value of high expression of PR was based on the positive nuclear staining of over 20% of the tumor cells[26]. The cutoff value of low expression of PR was based on the proportion of positive nuclear staining of tumor cells ≥ 1% and ≤ 20%[26]. The Her-2 status was considered positive if the IHC score was 3 + [17]. For Her-2 2 + expression, Her-2 status was determined with gene amplification by fluorescence in situ hybridization (FISH)[11,17]. Her-2 copy number > 6.0 or Her-2/CEP17 (chromosome enumeration probe-17) ratio > 2.0 was defined as Her-2 positive[17,28]. A Ki-67 proliferative index of > 20% was considered high[29].

Construction of prediction model

Of the 710 cases, there was only one male patient with breast cancer. This 1 case not only had no statistical significance in the total sample size of more than 700 cases, but also led to a decrease in the generalizability of the statistical results, so they were removed, and finally only 709 cases were included in the statistical data. Firstly, a random variable function was established for 709 cases of data included in the statistics. According to the quartile method, data less than 25% of the random number was defined as the validation set, and the remaining 75% of the data was defined as the development set. Then the stepwise regression method was used to screen out the variables with significant prediction efficiency from the development set, and the logical regression equation was obtained. The β value of each variable in the equation was the score of each variable, while the score of a variable that was not included in the equation was zero. The total score of each sample was calculated by summation. Next, the ROC curve was drawn using the verification set data to evaluate the prediction model. Finally, the prediction score of each sample was calculated by using the logical regression equation and arranged in the order from low to high. According to the order, the scores of all samples were equally divided into 5 segments, and each segment accounted for about 20%. The average metastatic probability of the sample in this segment was taken as the metastatic probability of the samples with this grade[30].

Data and statistical analysis

All statistical analyses were carried out using SAS9.4 international standard statistical programming software and the value of $p < 0.05$ was considered to be statistically significant. The enumeration data were described by frequency and percentage, the chi-square test was used for inter-group comparison; the median was used to describe the measurement data that did not meet the normal distribution, the t-test was used to determine whether there was any difference between the prediction results and the reference standard, and the nonparametric rank sum test was used for inter-group comparison. Risk factors were analyzed by binary logical regression analysis[30].

Nine variables were entered into the MSKCC website (www.mskcc.org/nomograms): tumor type, LVI, tumor size, tumor location, age, multifocality, and ER and PR status. Subsequently, the probability of ALN metastasis was calculated for each patient. A ROC curve was drawn, and the area under the curve (AUC) was calculated. An AUC value between 0.5 and 0.7 indicates that the model has a certain accuracy, between 0.7 and 0.9 indicates that it has a good accuracy, and when it is above 0.9 that it has a very high accuracy[31].

Results

General characteristics of the study population

Our study comprised 709 patients, 531 in the development set and 178 in the validation set. The descriptive characteristics of the development and validation sets are provided in Table 1. There was no significant difference between the development and validation sets. The rate of ALN metastasis in breast cancer patients was 51.22% (272/531) and 52.25% (93/178) within the development and validation sets, respectively. Based on the results of the univariate analysis, breast physical exam, tumor size on imaging, tumor location, abnormal calcification, ultrasound grades of ALNs, PR, Her-2 status, Ki-67 proliferative index, histological grade, LVI, NLR and PLR ($p < 0.05$) were significantly associated with the incidence of ALN metastasis. Multifocality was of borderline significance for predicting ALN metastasis ($p = 0.0579$).

Validation of the MSKCC model

A comparison between the verification populations from the MSKCC and our patient cohort is shown in Table 2. The descriptive characteristics of these two populations differ with respect to surgery. The patients in our validation population included SLNB and ALND patients. Therefore, we verified the predictive power of MSKCC for ALN but not SLN metastasis. We could not use the MSKCC model to predict the likelihood that patients diagnosed with breast cancer with skin changes or diagnosed with ductal carcinoma in situ with microinvasion (< 0.1 cm) have positive ALNs. Therefore, we could not compare the subtypes between the two populations. Additionally, we excluded those patients when validating the usefulness of the MSKCC model. We input each variable data online to obtain the probability of MSKCC for each patient's ALN metastasis and drew the ROC curve according to the real value and predicted value to assess the accuracy of the MSKCC model for predicting ALN metastasis in our cohort. As shown in Fig. 1a, the AUC value for the MSKCC model in our verification population was 0.817, and the 95% confidence interval (95% CI) was 0.784 to 0.851, which was significant ($p < 0.001$).

Establishment of the new prediction model

We developed a new prediction model to overcome the limitations of the preoperative application of the MSKCC model. The multiple logistic regression analysis revealed that physical exam ($p = 0.0034$), ultrasound grades of ALNs ($p < 0.0001$), Her-2 status ($p = 0.0176$) and LVI ($p < 0.0001$) were related to ALN metastasis in breast cancer and showed significant differences between groups. Associations between clinical data and ALN metastasis are listed in Table 3. The following regression model for predicting metastatic and nonmetastatic ALNs was obtained:

Characteristic	Development Set		Validation Set		*P* value
	No. of Patients (n = 531)	%	No. of Patients (n = 178)	%	
Sex					
Female	531	100	178	100	
Male	0	0	0	0	
Age, years					0.3127
Median	54		52		
Range	23–91		26–91		
Menstruation					0.8367
Menopause	273	51.4	85	47.7	
Peri-menopause	64	12.1	19	10.7	
Premenopausal	194	36.5	74	41.6	
Physical exam					< 0.0001
Negative	427	80.4	145	81.5	
Positive	104	19.6	33	18.5	
*Tumor size, cm**					< 0.0001
Median	2.3		2.49		
Range	0.4–11.4		0.57–13.0		
Laterality					0.3788
Right	250	47.1	86	48.3	
Left	281	52.9	92	51.7	
Tumor location					0.0001
UIQ	106	20.0	33	18.5	
LIQ	23	4.3	9	5.1	
LOQ	52	9.8	25	14.0	
UOQ	242	45.6	68	38.2	
CQ	68	12.8	26	14.6	
MQ	40	7.5	17	9.6	
Diffuse distribution					0.0623
Yes	38	7.2	18	10.1	
No	493	92.8	160	89.9	
Multifocality					0.0579
NO	447	84.2	145	81.5	
Yes	84	15.8	33	18.5	
Abnormal calcification					0.0067
Yes	110	20.7	49	27.5	
No	421	79.3	129	72.5	
NLR					0.0017
Median	1.99		2.05		
Range	0.37–24.84		0.80–9.14		
PLR					0.0101
Median	133.33		130.48		
Range	41.77–1017.65		53.59–372.86		
Histologic grade					0.0004
I	14	2.6	5	2.8	
II	387	72.9	131	73.6	
III	110	20.7	36	20.2	
Lobular	20	3.8	6	3.4	
Estrogen receptor					0.707
Negative	150	28.3	50	28.1	
Low expression	25	4.7	4	2.2	
High expression	356	67.0	124	69.7	
Progesterone receptor					0.0139
Negative	222	41.8	68	38.2	
Low expression	90	16.9	39	21.9	
High expression	219	41.3	71	39.9	
Her-2/neu					< 0.0001

Continued

Characteristic	Development Set		Validation Set		*P* value
	No. of Patients (n = 531)	%	No. of Patients (n = 178)	%	
Negative	387	72.9	132	74.2	
Positive	144	27.1	46	25.8	
Ki-67					< 0.0001
Low expression	271	51.0	89	50.0	
High expression	260	49.0	89	50.0	
Ultrasound grades of ALNs					< 0.0001
Negative	295	55.6	93	52.2	
Positive	236	44.4	85	47.8	
LVI					< 0.0001
Negative	300	56.5	95	53.4	
Positive	231	43.5	83	46.6	
ALN metastases					
Yes	272	51.2	93	52.2	
No	259	48.8	85	47.8	

Table 1. Descriptive characteristics of the development and validation sets. Note: *Tumor size was defined as the longest diameter of the mass measured by ultrasound. Abbreviations: UOQ, upper outer quadrant; LOQ, lower outer quadrant; UIQ, upper inner quadran; LIQ, lower inner quadrant; CQ, central quadrant; MQ, multiple quadrant; NLR, Neutrophils/Lymphocytes; PLR, Platelets/Lymphocytes; LVI, Lymphovascular invasion; ALN, axillary lymph nodal.

Risk of score = -2.2509 + 0.984 × physical exam (Negative: 0; Positive: 1) + 3.1703 × ultrasound grades of ALNs (Negative: 0; Positive: 1) + 0.6622 × Her-2 status (Negative: 0; Positive: 1) + 1.5287 × LVI status (Negative: 0; Positive: 1). The AUC value of the prediction model was 0.895, and the 95% CI was 0.867 to 0.923, which was statistically significant ($p < 0.001$) (Fig. 1b).

Establishment of the risk scoring system

A 5-grade risk-scoring system was developed. Table 4 indicates the risk of ALN metastasis according to the clinical data characteristics of breast cancer. In this scoring system, the probability of metastasis was 11.25% in ALNs without significantly suspicious metastatic clinical data (grades 1). In other words, the false-negative rate of the scoring system is 11.25%. Additionally, the Spearman rank correlation analysis of the grading and metastasis risk of the scoring system showed that the rank correlation coefficient was 1, $p < 0.0001$. This showed that, on the whole, the metastasis probability increased with increasing risk grade, and there was a positive correlation between them. The reference standard was taken as the state variable, the total score was taken as the test variable, the ROC curve was drawn to verify the regression equation based on the ROC curve, and finally, the critical value of -0.06 was obtained (the risk of metastasis was considered to be high if it was greater than -0.06 points). The AUC value of the risk scoring system was 0.887, and the 95% CI was 0.862 to 0.912 ($p < 0.001$), which was statistically significant (Fig. 1c). This finding shows that the transition from the prediction model to the scoring system was stable.

Prospective use of the risk scoring system

We randomly selected one-fourth of the total data as test data to internally validate the prediction model. As shown in Fig. 1d, the results showed that the scoring system performed well in the internal verification test (AUC: 0.865; [95% CI: 0.810 to 0.920]; $p < 0.001$). This finding shows that the model is suitable for use in routine clinical practice. Considering that the false-negative rate of SLNB averaged 8.4%, ranging from 0 to 29% across all trials. We divided the management recommendations on breast cancer patients' ALNs into three levels according to the false-negative rate and the critical value of the risk scoring system: consider exempting SLNB (Grade 1, metastasis risk approximately11.25%), consider SLNB (Grade 2, metastasis risk approximately 34.4%), and consider ALND (Grades 3,4 and 5, metastasis risk approximately 74.17- 93.46%).

Establishment of the network-based prediction model

An online automated scoring system was developed (https://pay-test.coalapay.cn/Coala/thyroid/BCD_EN.html; Fig. 2) using the clinical data characteristics significantly associated with ALN metastasis for the simplified calculation and summation of the scoring system for metastasis risk stratification. Through this online automated scoring system, applicants can easily obtain the risk of grade, probability of metastasis and related management recommendations for ALNs.

Discussion

The results of the present study can be summarized as follows. First, a simple and easily accessible, web-based, diagnostic scoring system was developed using clinical features, imaging, and pathological indices of breast tumors to stratify the metastatic risk and management of ALNs. Second, this scoring system showed excellent

	Wei Fang retrospective group			MSKCC, New York validation group		
		ALN (+)			SLN (+)	
Variable	No.	No.	%	No.	No.	%
No. of patients	613	296	48.3	1545	579	37.5
Age (years)						
≤ 40	70	42	60.0	181	88	48.6
41–69	473	233	49.3	1066	406	38.1
≥ 70	70	21	30.0	298	85	28.5
Tumor size (cm)						
T1mic	1	0	0	51	11	21.6
T1a	15	5	33.3	199	31	15.6
T1b	42	7	16.7	362	84	23.2
T1c	226	78	34.5	624	263	42.1
T2 ≤ 3	179	94	52.5	215	121	56.3
T2 > 3	125	90	72.0	80	56	70.0
T3	25	22	88.0	14	13	92.9
Tumor location						
UOQ	301	164	54.5	879	330	37.5
LOQ	80	36	45.0	211	91	43.1
UIQ	130	43	33.1	264	74	28.0
LIQ	33	17	51.5	135	49	36.3
Central	69	36	52.2	56	35	62.5
Histologic grade*						
I	15	1	6.7	97	11	11.3
II	449	210	46.8	375	139	37.1
III	125	75	60.0	810	346	42.7
Unknown	-	-	-	97	22	22.7
Tumor type						
Ductal	551	276	50.1	1339	514	38.4
Lobular	23	10	43.5	166	61	36.7
Special Type	39	10	25.6	40	4	10.0
LVI						
No	366	105	28.7	1205	344	28.5
Yes	247	191	77.3	340	235	69.1
Multifocality						
No	510	238	46.7	1155	403	34.9
Yes	103	58	56.3	390	176	45.1
ER						
Negative	182	92	50.5	273	99	36.3
Positive	431	204	47.3	1186	462	39.0
Unknown	-	-	-	86	18	20.9
PR						
Negative	302	156	51.7	600	219	36.5
Positive	311	140	45.0	858	342	39.9
Unknown	-	-	-	86	18	20.9

Table 2. Comparison of descriptive characteristics of the two validation groups of the MSKCC model for predicting ALN metastasis, New York and Wei Fang. Note: Tumor size was defined as the size of the invasive component, and the T classification was carried out according to the 2002 TNM classification system. In cases of multifocal tumors or unifocal tumors that involved more than 1 quadrant, the tumor location was classified in the following order of priority: UOQ, central quadrant (central), LOQ, LIQ, and UIQ. For example, a tumor in the UIQ and central quadrants would be classified as central. A tumor involving the central quadrant and UOQ would be classified as UOQ. If all quadrants were involved, the tumor was classified as UOQ. Positivity of estrogen and progesterone receptors was defined as at least 10% or more immunostained cells. Abbreviations: UOQ, upper outer quadrant; LOQ, lower outer quadrant; UIQ, upper inner quadrant; LIQ, lower inner quadrant; LVI, lymphovascular invasion; ER, estrogen receptor; PR, progesterone receptor. *Excluding lobular carcinomas.

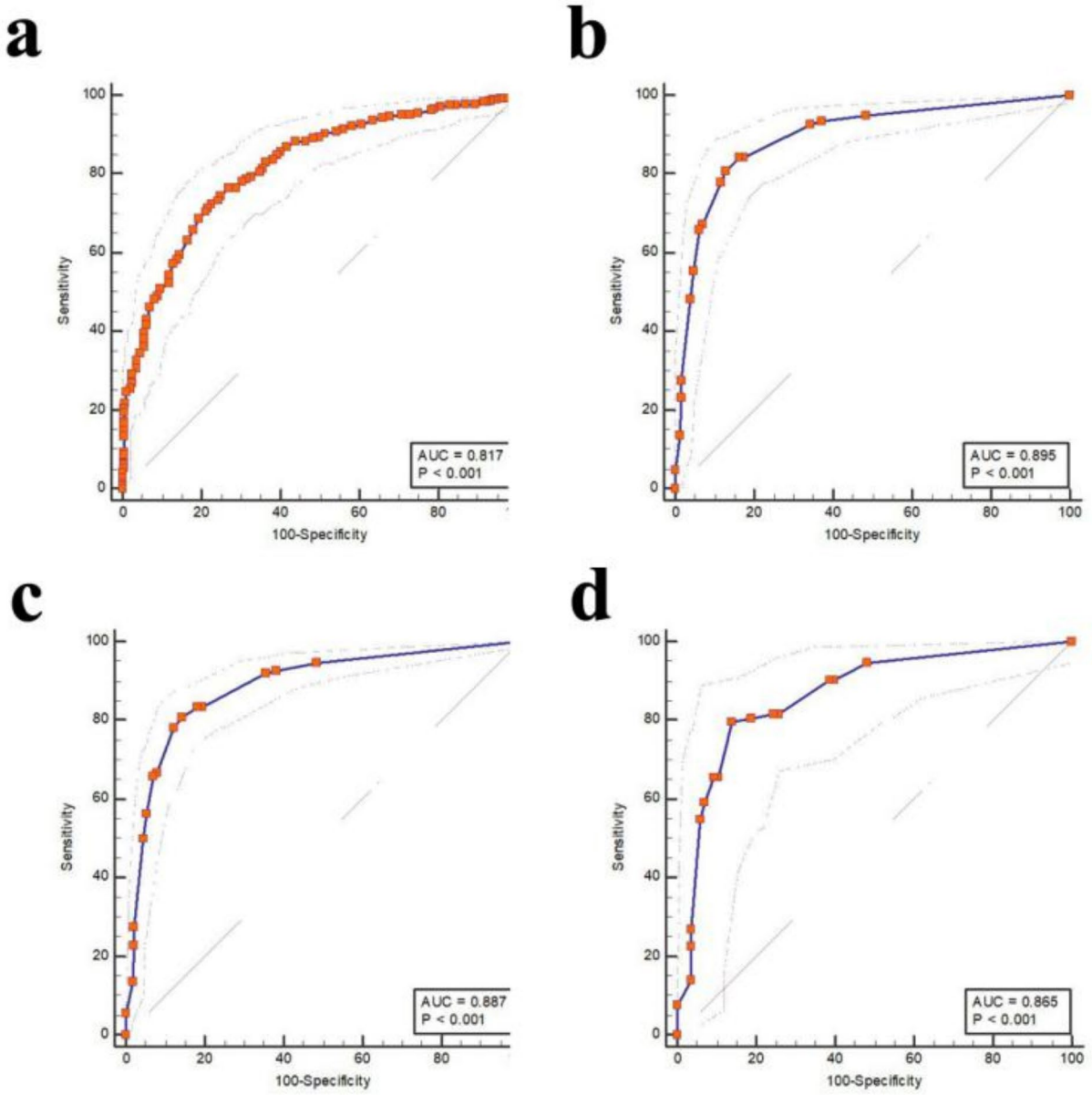

Fig. 1. The receiver operating characteristic (ROC) curve of the research. (**a**) Performance of the MSKCC model applied to the verification group (n = 613). The area under the ROC curve was 0.817, and the 95% confidence interval (95% CI) was 0.784–0.851, $p < 0.001$. (**b**) Performance of the new prediction model based on the development set (n = 531). The area under the ROC curve was 0.895, and the 95% confidence interval (95% CI) was 0.867–0.923, $p < 0.001$. (**c**) Performance of the novel scoring system based on the risk score (n = 709). The area under the ROC curve was 0.887, and the 95% confidence interval (95% CI) was 0.862–0.912, $p < 0.001$. (**d**) Performance of the validation set (n = 178). The area under the ROC curve was 0.865, and the 95% confidence interval (95% CI) was 0.810–0.920, $p < 0.001$.

predictive accuracy with an AUC of approximately 0.9 in the development set. In routine clinical practice, this web-based scoring system can automatically calculate and estimate the risk of ALN metastasis and provide corresponding management recommendations.

In clinical practice, accurate preoperative evaluation and management of ALNs is the key to providing accurate individualized diagnosis and treatment for breast cancer patients[32–34]. To achieve this goal, scholars from numerous medical centers have studied ALN metastasis in breast cancer and developed relevant prediction models based on either tumor pathological features or radiomic characteristics of the tumor[11,15–17,33]. However, these models have the characteristics of incomplete coverage of predictive variables, high costs, procedural complexity, and inability to popularize, which limits their clinical application[12,18].

Clinical data	nonmetastatic ALNs (n = 259)	metastatic ALNs (n = 272)	*p*-Value	OR[95%CI]	Score
Physical exam					
Negative	238 (91.9)	189 (69.5)	Reference	Reference	0
Positive	21 (8.1)	83 (30.5)	0.0034	2.68(1.39–5.16)	0.984
Her-2/neu					
Negative	211 (81.5)	176 (64.7)	Reference	Reference	0
Positive	48 (18.5)	96 (35.3)	0.0176	1.94(1.12–3.35)	0.6622
Ultrasound grades of ALNs					
Negative	231 (89.2)	64 (23.5)	Reference	Reference	0
Positive	28 (10.8)	208 (76.5)	< 0.0001	23.82(14.11–40.2)	3.1703
LVI					
Negative	191 (73.7)	109 (40.1)	Reference	Reference	0
Positive	68 (26.3)	163 (59.9)	< 0.0001	4.61(2.79–7.61)	1.5287

Table 3. Clinical data characteristics of multifactor analysis and estimation of the metastasis risk of the development dataset.

Risk of Grade	Risk of Score	Metastasis risk (%)		
		Score system (%; [metastasis n/total n])	Development set (%; [metastasis n/total n])	Validation set (%; [metastasis n/total n])
1	≦ -1.5887	11.25 (27/240)	10.00 (18/180)	15.00 (9/60)
2	-1.5887 < score ≦ -0.06	34.40 (43/125)	34.69 (34/98)	33.33 (9/27)
3	-0.06 < score ≦ 1.5816	74.17 (89/120)	76.67 (69/90)	66.67 (20/30)
4	1.5816 < score ≦ 2.4481	90.60 (106/117)	90.48 (76/84)	90.91 (30/33)
5	2.4481 < score	93.46 (100/107)	94.94 (75/79)	89.29 (25/28)
Total		51.48 (365/709)	51.22 (272/531)	52.25 (93/178)

Table 4. Metastatic risk of ALNs according to the novel scoring system, development set, and validation set.

To overcome these drawbacks, we referred to the establishment method of the MSKCC model and developed a network based prediction model that combines physical exam, ultrasound grades of ALNs, Her-2 status and LVI (Tables 1 and 3). Generally, a model that performs with an AUC value of 0.7–0.8 is considered good, whereas values of 0.81–0.90 are considered excellent[31]. As shown in Fig. 1b, by analyzing the ROC curve of the prediction model, we obtained an AUC value of 0.895. This indicated that the prediction model we constructed in this study showed excellent predictability. Furthermore, when we selected the clinical data of another 178 patients to validate the prediction model internally, the results showed excellent prediction accuracy, and the AUC value of the internal validation set was 0.865 (Fig. 1d). The AUC values in these two populations were both greater than 0.754 of the original MSKCC model, indicating that our constructed model was more accurate[15]. Meanwhile, in comparison to prediction models developed by other research centers, such as the MSKCC model, the SCH model, etc., our proposed model was simpler to use since only four variables were included versus the nine variables in the MSKCC model and the five variables in the SCH model[15,16,35]. Although the prediction model in this study only includes four variables, these four variables come from three different prediction directions, making the prediction content more comprehensive. In addition, when we applied the MSKCC model to the retrospective data from our center to predict the probability of ALN metastasis, the AUC value was 0.817 (Fig. 1a and Table 2). Although this value is larger than the original MSKCC result of 0.754, it is still lower than the result of our prediction model of 0.895. We suspect that the reason for this result may be potentially related to skipping metastasis of ALNs. The analysis results not only provide indirect validation of the MSKCC model's accuracy using external data, but also affirm the superiority of our prediction model.

According to an investigation report from the American Society of Clinical Oncology (ASCO), the overall false-negative rate for SLNB was 8.4%, with a range of 0–29%[36]. Therefore, taking into account the potential risks and benefits of surgery, if surgeons are willing to accept a false-negative rate ranging from 0 to 29%, patients in the low-risk metastasis group may be considered for exemption from ALN surgery. Furthermore, to enhance the clinical practicability of the predictive model, we developed a risk scoring system with five grades. Each suspicious clinical characteristic related to ALNs metastasis was assigned a different risk score, and the risk of metastasis was determined by calculating the total score. As shown in Fig. 1c, the ROC curve analysis of the risk scoring system yielded an AUC value of 0.887, indicating that the transition from the prediction model to the scoring system was stable and reliable. After calculating the metastasis probabilities for different grades in the scoring system, we found that the ALN metastasis probability for grade 1 was 11.25%, which fell within the false-negative rate range of SLNB (Table 4). Therefore, in clinical practice, we suggest that exemption from ALN surgery can be considered for patients in the grade 1 category. Previously, several studies indicated that SLNB could be avoided when the MSKCC predictive value was ≤ 10%; however, the application of this criterion was limited due to the low proportion of patients who benefit from it within the overall SLNB population (7.7%)[16,31].

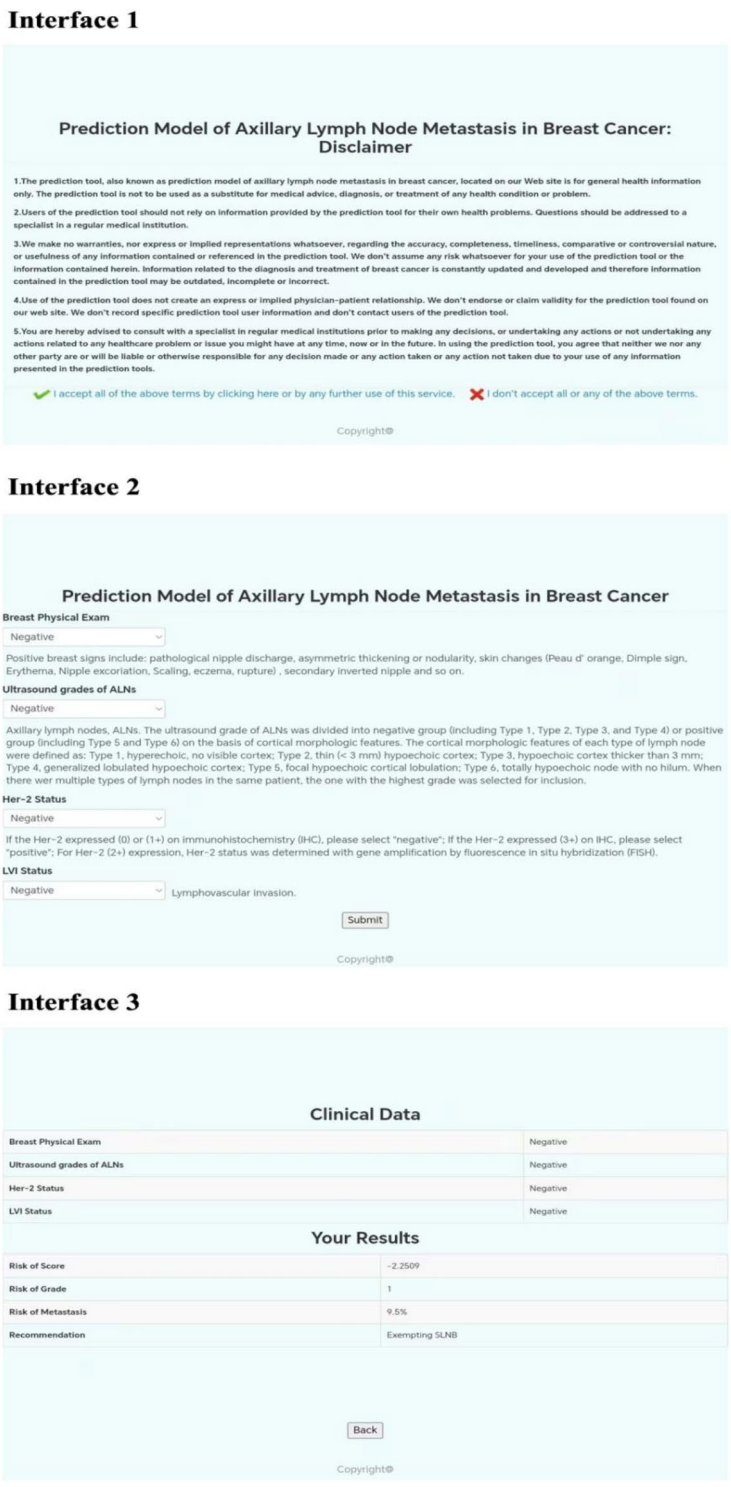

Fig. 2. Online risk calculation system. An online resource is available at https://pay-test.coalapay.cn/Coala/thyroid/BCD_EN.html for the easy calculation and summation of the metastasis risk stratification of ALNs using the clinical data characteristics of breast cancer.

In this study, patients with low metastatic risk (grade 1 segments) accounted for 33.85% of all patients in our proposed model. In other words, more people could benefit from our proposed model. In addition, the results of Spearman's correlation coefficient for ranked data between the risk grade and the metastasis probability showed that, on the whole, the metastasis probability increased with increasing risk grade, and there was a positive correlation between them. By analyzing the ROC curve of the scoring system, we obtained a critical value of

-0.06 points. Statistically, if the risk score of a case was greater than -0.06 points (the corresponding metastasis probability was approximately 34%), it was considered ALN metastasis[37]. Thus, combined with the metastasis probability of each risk grade shown in Table 4, we further categorized grades 2 as belonging to a medium-risk group (where SLNB was recommended), and grades 3 and above as falling into a high-risk group (where ALND was recommended). This approach provides more intuitive help for clinical workers making clinical decisions.

To facilitate clinical application, we have developed an easily accessible online risk calculator (https://pay-test.coalapay.cn/Coala/thyroid/BCD_EN.html). This tool automates the scoring system's calculation, thereby enhancing its usability and intuitiveness in clinical settings. All users are free to utilize this risk calculator online and can further validate our scoring system with external datasets. This accurate and practical model predicts the likelihood of ALN metastasis, guiding clinical decision-making effectively.

Our study has some notable strengths and limitations. The strengths of this study can be summarized as follows. Comprehensiveness: The parameters of the prediction model encompass clinical examination, imaging, and histopathological findings, providing a comprehensive reflection of ALN status in breast cancer patients. Convenience: The model is freely accessible on the website, and clinical practitioners can easily input relevant prediction parameters to obtain automatic calculation of the prediction results. Intuitiveness: The risk stratification, probability of metastasis, and management recommendations for ALN metastasis are presented in a concise report format, making them clear and easily understandable. However, our research also has some limitations. First, this study is a single-center experimental study. The development set data and the validation set data were randomly selected from the total samples using the method of random function variables, ensuring no selection bias between them. To ensure the accuracy of the prediction model, the sample size of the development set was larger, specifically three times that of the validation set. Additionally, both the development set and validation set data originated from the same research center, meaning the validation set only served as internal validation. Therefore, we cannot ascertain whether these patients are representative of the general population. Fortunately, we included a larger sample size to mitigate any potential selection bias, and the risk scoring system we developed is freely available on our website, allowing researchers from other centers to use their data for external validation of our scoring system.Second, the potential for interobserver variability in the interpretation of pathological findings between the two pathologists was not assessed. However, given that the pathologists involved in this study had over 10 years of clinical experience in diagnosing breast cancer, the results may be more reproducible than if they had been evaluated by pathologists with less experience.

In conclusion, this study presents an accurate, comprehensive, and user-friendly multivariate prediction model along with an online risk calculator. This model will enable a true representation of the risk of ALN metastasis in breast cancer patients before surgery, thereby facilitating the selection of appropriate surgical protocols tailored to individual patients. It is worth noting that the universal applicability of this prediction model requires confirmation in future multicenter experimental studies with large cohorts that represent the general population. Until the prediction model is further evaluated, this predictive tool should be used with caution when deciding not to perform an ALN surgery in patients with a low risk of ALN metastasis.

Data availability

Data is available from the corresponding author on reasonable request.

Received: 10 February 2024; Accepted: 30 December 2024
Published online: 09 January 2025

References

1. Banerjee, M., George, J., Song, E. Y., Roy, A. & Hryniuk, W. Tree-based model for breast cancer prognostication. *J Clin Oncol.* **22**, 2567–2575. https://doi.org/10.1200/JCO.2004.11.141 (2004).
2. Loibl, S. et al. Early breast cancer: ESMO Clinical Practice Guideline for diagnosis, treatment and follow-up. *Ann. Oncol.* **35**, 159–182. https://doi.org/10.1016/j.annonc.2023.11.016 (2024).
3. Gradishar, W. J. et al. Breast cancer, version 3.2024, NCCN clinical practice guidelines in oncology. *J. Natl. Compr. Cancer Netw.* **22**, 331–357. https://doi.org/10.6004/jnccn.2024.0035 (2024).
4. Boguševičius, A. & Čepulienė, D. Quality of life after sentinel lymph node biopsy versus complete axillary lymph node dissection in early breast cancer: A 3-year follow-up study. *Medicina (Kaunas)* **49**, 111–117 (2013).
5. Krag, D. N. et al. Technical outcomes of sentinel-lymph-node resection and conventional axillary-lymph-node dissection in patients with clinically node-negative breast cancer: Results from the NSABP B-32 randomised phase III trial. *Lancet Oncol.* **8**, 881–888. https://doi.org/10.1016/S1470-2045(07)70278-4 (2007).
6. Gentilini, O. & Veronesi, U. Abandoning sentinel lymph node biopsy in early breast cancer? A new trial in progress at the European Institute of Oncology of Milan (SOUND: Sentinel node vs Observation after axillary UltraSouND). *Breast* **21**, 678–681. https://doi.org/10.1016/j.breast.2012.06.013 (2012).
7. van Roozendaal, L. M. et al. Clinically node negative breast cancer patients undergoing breast conserving therapy, sentinel lymph node procedure versus follow-up: A Dutch randomized controlled multicentre trial (BOOG 2013–08). *BMC Cancer* **17**, 459. https://doi.org/10.1186/s12885-017-3443-x (2017).
8. Reimer, T. et al. Restricted axillary staging in clinically and sonographically node-negative early invasive breast cancer (c/iT1-2) in the context of breast conserving therapy: First results following commencement of the Intergroup-Sentinel-Mamma (INSEMA) Trial. *Geburtshilfe Frauenheilkd.* **77**, 149–157. https://doi.org/10.1055/s-0042-122853 (2017).
9. Clinical trials. gov. Sentinel Node Biopsy Vs Observation After Axillary PET. https://clinicaltrials.gov/ct2/show/NCT04072653.
10. Pusztai, L. et al. Event-free survival by residual cancer burden with pembrolizumab in early-stage TNBC: exploratory analysis from KEYNOTE-522. *Ann. Oncol.* **35**, 429–436. https://doi.org/10.1016/j.annonc.2024.02.002 (2024).
11. Xue, M. et al. Nomogram based on breast MRI and clinicopathologic features for predicting axillary lymph node metastasis in patients with early-stage invasive breast cancer: A retrospective study. *Clin. Breast Cancer* **22**, e428–e437. https://doi.org/10.1016/j.clbc.2021.10.014 (2022).
12. Britton, P. et al. Measuring the accuracy of diagnostic imaging in symptomatic breast patients: Team and individual performance. *Br. J. Radiol.* **85**, 415–422. https://doi.org/10.1259/bjr/32906819 (2012).

13. Winkler, N. et al. Comparison of diagnostic sensitivity and procedure-related pain of concurrent ultrasound-guided fine-needle aspiration and core-needle biopsy of axillary lymph nodes in patients with suspected or known breast cancer. *J. Breast Imaging* **5**, 436–444. https://doi.org/10.1093/jbi/wbad031 (2023).
14. Sallout, L. et al. Fine-needle aspiration biopsy of axillary lymph nodes: A reliable diagnostic tool for breast cancer staging. *Cancer Cytopathol.* **132**, 103–108. https://doi.org/10.1002/cncy.22770 (2024).
15. Bevilacqua, J. L. et al. Doctor, what are my chances of having a positive sentinel node? A validated nomogram for risk estimation. *J. Clin. Oncol.* **25**, 3670–3679. https://doi.org/10.1200/JCO.2006.08.8013 (2007).
16. Chen, J. Y. et al. Predicting sentinel lymph node metastasis in a Chinese breast cancer population: assessment of an existing nomogram and a new predictive nomogram. *Breast Cancer Res. Treat.* **135**, 839–848. https://doi.org/10.1007/s10549-012-2219-x (2012).
17. Cheng, J. et al. Development of high-resolution dedicated PET-based radiomics machine learning model to predict axillary lymph node status in early-stage breast cancer. *Cancers (Basel)* **14**, 950. https://doi.org/10.3390/cancers14040950 (2022).
18. Liu, D. et al. Models for predicting sentinel and non-sentinel lymph nodes based on pre-operative ultrasonic breast imaging to optimize axillary strategies. *Ultrasound Med. Biol.* **47**, 3101–3110. https://doi.org/10.1016/j.ultrasmedbio.2021.06.014 (2021).
19. Berraondo, P. et al. Innate immune mediators in cancer: between defense and resistance. *Immunol. Rev.* **274**, 290–306. https://doi.org/10.1111/imr.12464 (2016).
20. Singla, T., Singla, G., Ranga, S., Singla, S. & Arora, R. Role of platelet aggregation in metastatic breast cancer patients. *Indian J. Pathol. Microbiol.* **63**, 564–569. https://doi.org/10.4103/IJPM.IJPM_817_19 (2020).
21. Challa, B. et al. Artificial intelligence-aided diagnosis of breast cancer lymph node metastasis on histologic slides in a digital workflow. *Mod. Pathol.* **36**, 100216. https://doi.org/10.1016/j.modpat.2023.100216 (2023).
22. Zheng, X. et al. Deep learning radiomics can predict axillary lymph node status in early-stage breast cancer. *Nat. Commun.* **11**, 1236. https://doi.org/10.1038/s41467-020-15027-z (2020).
23. Li, P. et al. Lung mesenchymal cells elicit lipid storage in neutrophils that fuel breast cancer lung metastasis. *Nat. Immunol.* **21**, 1444–1455. https://doi.org/10.1038/s41590-020-0783-5 (2020).
24. SenGupta, S., Subramanian, B. C. & Parent, C. A. Getting TANned: How the tumor microenvironment drives neutrophil recruitment. *J. Leukoc Biol.* **105**, 449–462. https://doi.org/10.1002/JLB.3RI0718-282R (2019).
25. Bedi, D. G. et al. Cortical morphologic features of axillary lymph nodes as a predictor of metastasis in breast cancer: in vitro sonographic study. *AJR Am. J. Roentgenol.* **191**, 646–652. https://doi.org/10.2214/AJR.07.2460 (2008).
26. Chinese Anti-Cancer Association, Committee of Breast Cancer Society (CACA-CBCS). Guidelines and norms for diagnosis and treatment of Breast Cancer in China Anti-Cancer Association (2017 version). *China Oncol.* **27**, 695–759 (2017). https://doi.org/10.19401/j.cnki.1007-3639.2017.09.004.
27. China Anti-Cancer Association. Guidelines for standardized practice of sentinel lymph node biopsy in breast cancer (2022 abridged version). *Chin. J. Clin. Oncol.* **49**, 1136–1142. https://doi.org/10.12354/j.issn.1000-8179.2022.20221052 (2022).
28. Wolff, A. C. et al. Recommendations for human epidermal growth factor receptor 2 testing in breast cancer: American Society of Clinical Oncology/College of American Pathologists clinical practice guideline update. *J. Clin. Oncol.* **31**, 3997–4013. https://doi.org/10.1200/JCO.2013.50.9984 (2013).
29. Goldhirsch, A. et al. Personalizing the treatment of women with early breast cancer: Highlights of the St Gallen International Expert Consensus on the Primary Therapy of Early Breast Cancer 2013. *Ann. Oncol.* **24**, 2206–2223. https://doi.org/10.1093/annonc/mdt303 (2013).
30. Shao, G. et al. Preoperative comprehensive malignancy risk estimation for thyroid nodules: Development and verification of a network-based prediction model. *Eur. J. Surg. Oncol.* **48**, 1264–1271. https://doi.org/10.1016/j.ejso.2022.03.016 (2022).
31. Klar, M. et al. Good prediction of the likelihood for sentinel lymph node metastasis by using the MSKCC nomogram in a German breast cancer population. *Ann. Surg. Oncol.* **16**, 1136–1142. https://doi.org/10.1245/s10434-009-0399-3 (2009).
32. Chang, J. M., Leung, J. W. T., Moy, L., Ha, S. M. & Moon, W. K. Axillary nodal evaluation in breast cancer: State of the art. *Radiology* **295**, 500–515. https://doi.org/10.1148/radiol.2020192534 (2020).
33. Marino, M. A., Avendano, D., Zapata, P., Riedl, C. C. & Pinker, K. Lymph node imaging in patients with primary breast cancer: Concurrent diagnostic tools. *Oncologist* **25**, e231–e242. https://doi.org/10.1634/theoncologist.2019-0427 (2020).
34. Cardoso, F. et al. 5th ESO-ESMO international consensus guidelines for advanced breast cancer (ABC 5). *Ann. Oncol.* **31**, 1623–1649. https://doi.org/10.1016/j.annonc.2020.09.010 (2020).
35. Dihge, L., Ohlsson, M., Edén, P., Bendahl, P. O. & Rydén, L. Artificial neural network models to predict nodal status in clinically node-negative breast cancer. *BMC Cancer* **19**, 610. https://doi.org/10.1186/s12885-019-5827-6 (2019).
36. Lyman, G. H. et al. American Society of Clinical Oncology guideline recommendations for sentinel lymph node biopsy in early-stage breast cancer. *J. Clin. Oncol.* **23**, 7703–7720. https://doi.org/10.1200/JCO.2005.08.001 (2005).
37. Breitbach, G. P. et al. Preoperative morphological diagnosis of axillary lymph nodes in a breast center consultation service: Evaluation of fine-needle aspiration and core biopsy techniques. *Arch. Gynecol. Obstet.* **300**, 1659–1670. https://doi.org/10.1007/s00404-019-05331-5 (2019).

Author contributions

B.Q.S. and G.D.S. convinced and designed the study, collected and analyzed data and contributed to the writing. M.M.S. and Z.G.S. reviewed data and literature. X.L.W., Y.N.S., Z.S., Z.J.J., C.H.X. and G.L.L. participated in the data collection and management. All authors read and approved the final manuscript.

Funding

This research was funded by grants from the Projects of Medical and Health Technology Development Program in Shandong Province (No. 202207020877; No. 202403061141), the Research Project of Weifang Municipal Health Commission (No. WFWSJK-2022-164) and the Weifang Science and Technology Development Program (No. 2024YX130). The funders had no role in the study design, data collection, analysis, publication decisions, or manuscript preparation.

Declarations

Competing interests

The authors declare no competing interests.

Consent to publish

Patients signed informed consent regarding publishing their data.

Additional information

Correspondence and requests for materials should be addressed to G.S.

Reprints and permissions information is available at www.nature.com/reprints.

Publisher's note Springer Nature remains neutral with regard to jurisdictional claims in published maps and institutional affiliations.